Table of Contents

List of Abbreviations

CNT	-	Carbon nanotube
SWNT	-	Single-walled nanotube
MWNT	-	Multi-walled nanotube
DWNT	-	Double-walled nanotube
FESEM	-	Field-emission scanning electron microscopy
CVD	-	Chemical vapour deposition
PECVD	-	Plasma enhanced chemical vapour deposition

Figure Captions

Figure 1: Various allotropes of carbon: (a) diamond, (b) fullerene, (c) multilayer fullerene, (d) single-walled carbon nanotube, (e) double-walled carbon nanotube, (f) multi-walled carbon nanotube and (g) graphene.

Figure 2: Graphene, the building block of all graphitic forms, can be wrapped to form the 0-D bucky balls, rolled to form the 1-D nanotubes and stacked to form the 3-D graphite.

Figure 3: (a) Schematic of the honeycomb structure of a graphene sheet (b) SWCNTs can be formed by folding the sheet along the shown lattice vectors leading to armchair, zigzag and chiral tubes.

Figure 4: Schematic diagram of single hot-zone pyrolysis assisted chemical vapor deposition setup.

Figure 5: Temperature profile of the furnace used for the pyrolysis.

Figure 6: FESEM images of as-prepared MWNTs synthesized at different temperatures (a) 750°C; (b) 800°C; (c) 850°C and (d) 900°C.

Figure 7. Typical cross-section of the vertically grown carbon nanotubes.

Figure 8. A typical Raman spectrum of multi-walled carbon nanotubes prepared at 850°C.

Figure 9. FESEM images of (a) as-prepared CNT at 850°C; (b) after oxidation at 500°C and (c) after chemical etching with HNO_3.

Figure 10. FESEM images of pure MWNTs prepared at different temperatures (a) 750°C; (b) 800°C; (c) 850°C and (d) 900°C.

Figure 11. Typical Raman spectrum of purified CNT for the sample prepared at 850°C.

Abstract

Multi-walled carbon nanotube (MWNT) and combination of single-walled (SWNT) and MWNT were synthesized using pyrolysis assisted chemical vapor deposition method. A single hot zone furnace was used for the synthesis of carbon nanotubes at various temperatures in the range of 750-900°C. The as-prepared CNT consisted of carbonaceous impurities and traces of transition metal contents. The as-prepared CNT was oxidized at 500°C and then treated with hydrochloric acid which resulted in pure CNT with a purity of 95%. The carbon nanotubes were characterized using field emission scanning electron microscopy (FESEM) and micro-Raman spectroscopy techniques. FESEM images clearly showed the presence of carbon nanotubes and the diameters of the MWNT prepared at various temperatures were in the range of 35-100 nm. The Raman spectroscopy data also showed the presence of D, G and 2D peaks which confirm the presence of CNT.

1. Introduction

Carbon (C) is the sixth element of the periodic table and has the lowest atomic number of any element in column IV of the periodic table. Carbon-based materials are exceptional mainly due to the various possible electronic configurations of the carbon atom known as the hybridization of atomic orbitals. Each carbon atom has six electrons which occupy 1*s*, 2*s* and 2*p* atomic orbitals [1]. The 1*s* orbital contains two strongly bound core electrons. Four weakly bound electrons occupy the 2*s* and 2*p* valence orbitals. In the crystalline phase, the valence electrons give rise to 2*s*, $2p^x$, $2p^y$ and $2p^z$ orbitals which are important in forming covalent bonds in carbon materials. Since the energy difference between the upper 2*p* energy levels and the lower 2*s* level in carbon is small compared to the binding energy of the chemical bonds, the electronic wave functions for these four electrons can readily mix with each other. This leads to change in the occupation of the 2*s* and three 2*p* atomic orbitals thereby enhancing the binding energy of the C atom with its neighbouring atoms [1].

The general mixing of 2*s* and 2*p* atomic orbitals is called hybridization, whereas the mixing of a single 2*s* electron with one, two, or three 2*p* electrons is called sp^n hybridization with n = 1,2,3. Thus three possible hybridizations occur in carbon: *sp*, sp^2 and sp^3, while other group IV elements such as Si and Ge exhibit primarily sp^3 hybridization. Carbon differs from Si and Ge in that carbon does not have inner atomic orbitals, except for the spherical 1*s* orbitals, and the absence of nearby inner orbitals facilitates hybridizations involving only valence *s* and *p* orbitals for carbon. The various bonding states are connected with certain structural arrangements, so that *sp* bonding gives rise to chain structures, sp^2 bonding to planar structures and sp^3 bonding to tetrahedral structures [1].

The formation of a particular allotrope of carbon is determined by the specific hybridization of carbon and its bonding to the surrounding atoms. The various allotropes of

carbon are shown in Figure 1 [2]. Carbon with sp^3 hybridization will form a tetrahedral lattice, giving rise to the diamond structure. Carbon with sp^2 hybridization will form graphite (arranged in hexagonal sheets), buckminsterfullerene (60 carbon atoms forming a sphere), or carbon nanotubes (long hollow tubes of carbon) depending on the conditions in which it is formed. Diamond and graphite have been known since ancient times, fullerene and CNTs were discovered two decades ago. On the other hand, graphene has been discovered recently and are just beginning to be characterized.

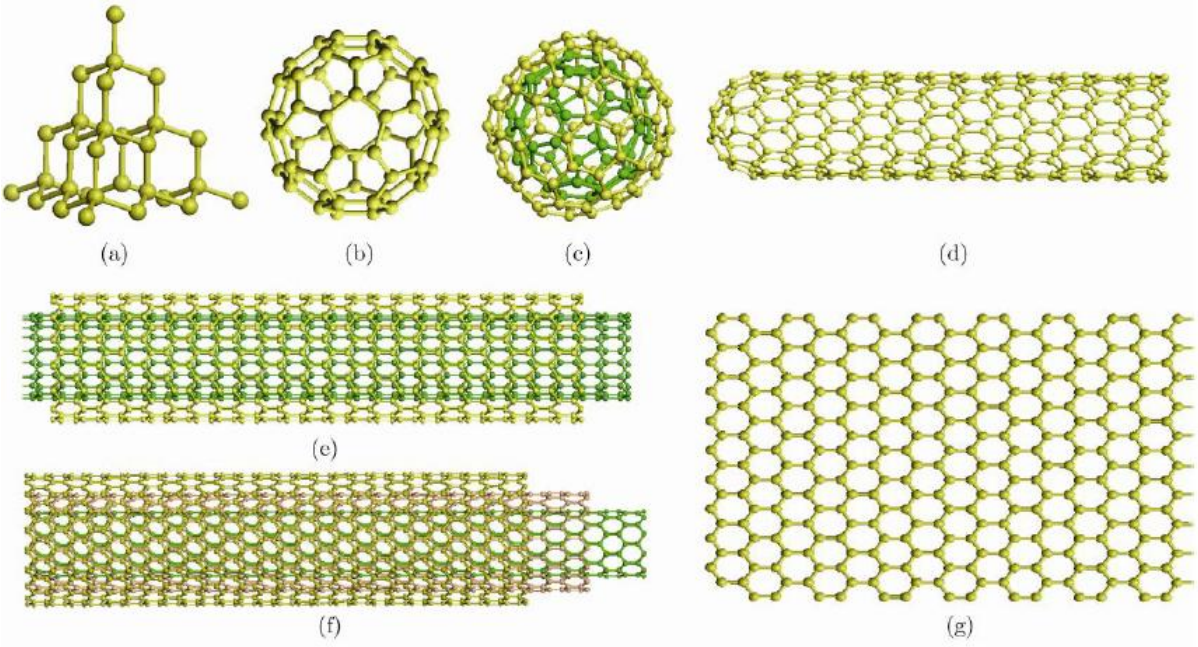

Figure 1: Various allotropes of carbon: (a) diamond, (b) fullerene, (c) multilayer fullerene, (d) single-walled carbon nanotube, (e) double-walled carbon nanotube, (f) multi-walled carbon nanotube and (g) graphene.

Graphene is the building block for various allotropes of carbon such as fullerene (zero dimensional), carbon nanotubes (one dimensional) and graphite (three dimensional) as shown schematically in Figure 2 [3]. For example, graphite (3-D carbon allotrope) is made of graphene sheets stacked on top of each. Fullerenes (buckyballs), can be made by wrapping a section of the graphene sheet. The 1-D carbon allotropes, carbon nanotubes (CNT) and

nanoribbons, can be made by rolling and slicing graphene sheets, respectively. In reality, however, these carbon allotropes are not synthesized from graphene.

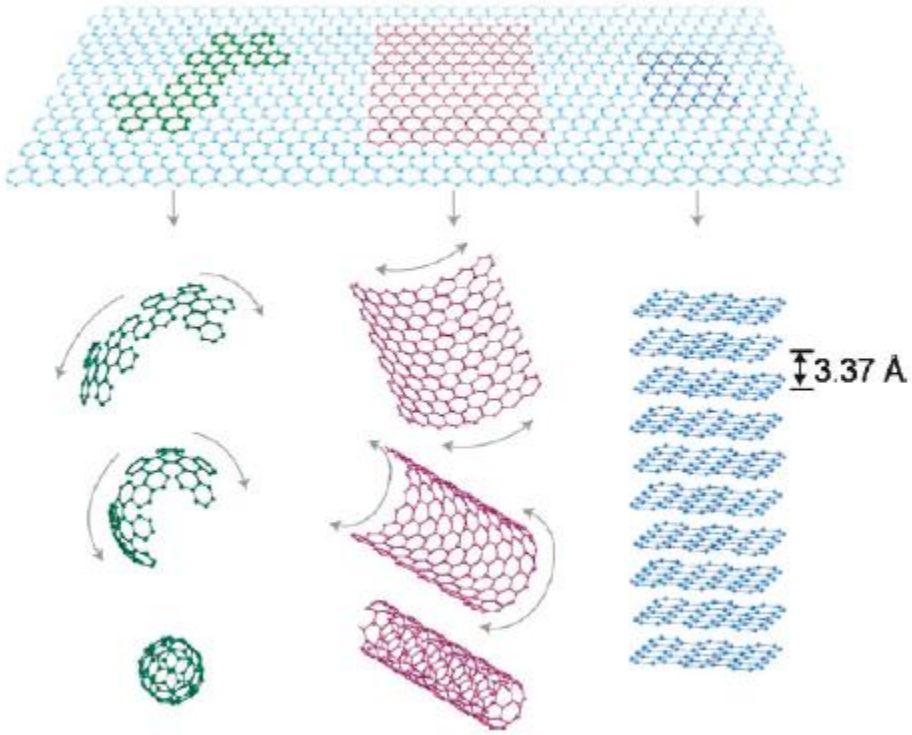

Figure 2: Graphene, the building block of all graphitic forms, can be wrapped to form the 0-D bucky balls, rolled to form the 1-D nanotubes and stacked to form the 3-D graphite.

The properties of carbon nanotubes depend on how the tubes are rolled up. CNT is characterized by a vector 'C_h' in terms of a set of two integers (n, m) corresponding to graphite vectors a_1 and a_2 (Figure 3) [1],

$$\mathbf{C_h = na_1 + ma_2} \qquad (1)$$

The CNT with m = n are commonly referred to as armchair tubes, those with m = 0 or n = 0 as zigzag tubes and others are called chiral tubes. For armchair and zigzag tubes, the chiral angles are 30 and 0°, respectively and other angles correspond to chiral tubes. The chiral angle 'θ' is defined as the angle between the vector C and the zigzag direction 'a_1', as shown in Figure 3. All armchair SWNTs are metals; those with n-m = 3j, where j is a non-zero

integer are small band gap semiconductors and all others are semiconductors with a band gap that inversely depends on the nanotube diameter.

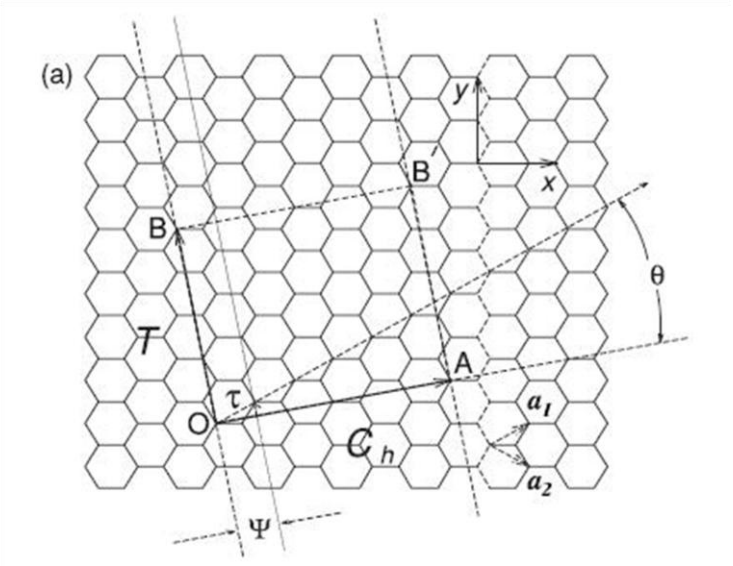

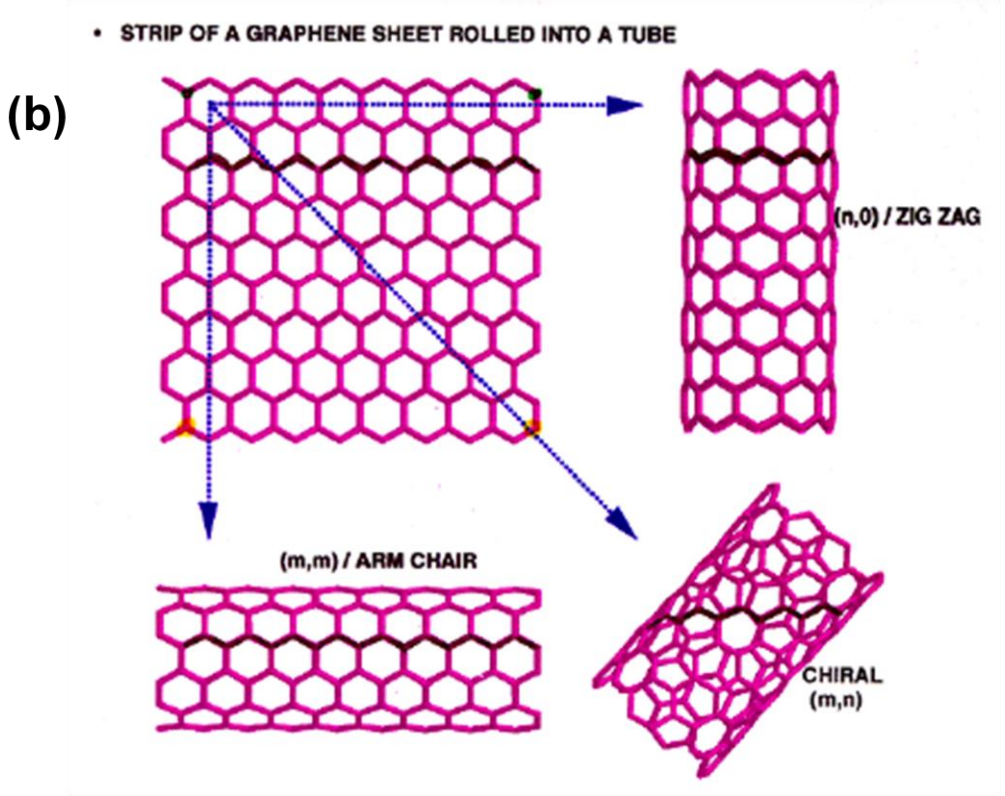

Figure 3: (a) Schematic of the honeycomb structure of a graphene sheet (b) SWCNTs can be formed by folding the sheet along the shown lattice vectors leading to armchair, zigzag and chiral tubes.

CNTs have remarkable electronic, optical, optoelectronic, mechanical, magnetic and electrical properties [4-8]. However, the electronic and optical properties of CNT are the most interesting for future nanotechnologies [9,10]. The carbon nanotubes have novel electronic properties because of their one-dimensional electronic structure and can carry high currents with essentially no heating. The novel electronic properties combined with their nanometer dimensions have made CNTs extremely attractive for applications in the field of nanoelectronics, energy as well as for sensor applications. In addition to this, CNTs can emit light at different wavelengths depending on their structure [11].

Various methods such as arc discharge [12], laser ablation [13], chemical vapour deposition (CVD) [14], plasma enhanced CVD [15], laser assisted CVD [16], aersol method [17], solvothermal method [18] and high pressure CO disproportionation process [19] have been used to synthesize single walled and multi-walled carbon nanotubes. For industrial applications, simple and cost effective production of CNTs is required. Nanda et al. proposed a new pyrolysis technique for the synthesis of CNTs [20]. In this method, no precursor gas is used and is a single step process. In this work, single step pyrolysis technique was used to develop carbon nanotubes. The CNTs were characterized using field emission scanning electron microscopy (FESEM) and micro-Raman spectroscopy techniques.

2. Experimental details

The synthesis of CNT has been carried out using pyrolysis assisted CVD technique consisting of single hot zone instead of double hot zone in the regular CVD method. The schematic diagram and the temperature profile of the furnace are shown in Figures 4 and 5, respectively. Benzene was used as the carbon source material and ferrocene as a source of iron which acted as a catalyst for the growth of CNTs.

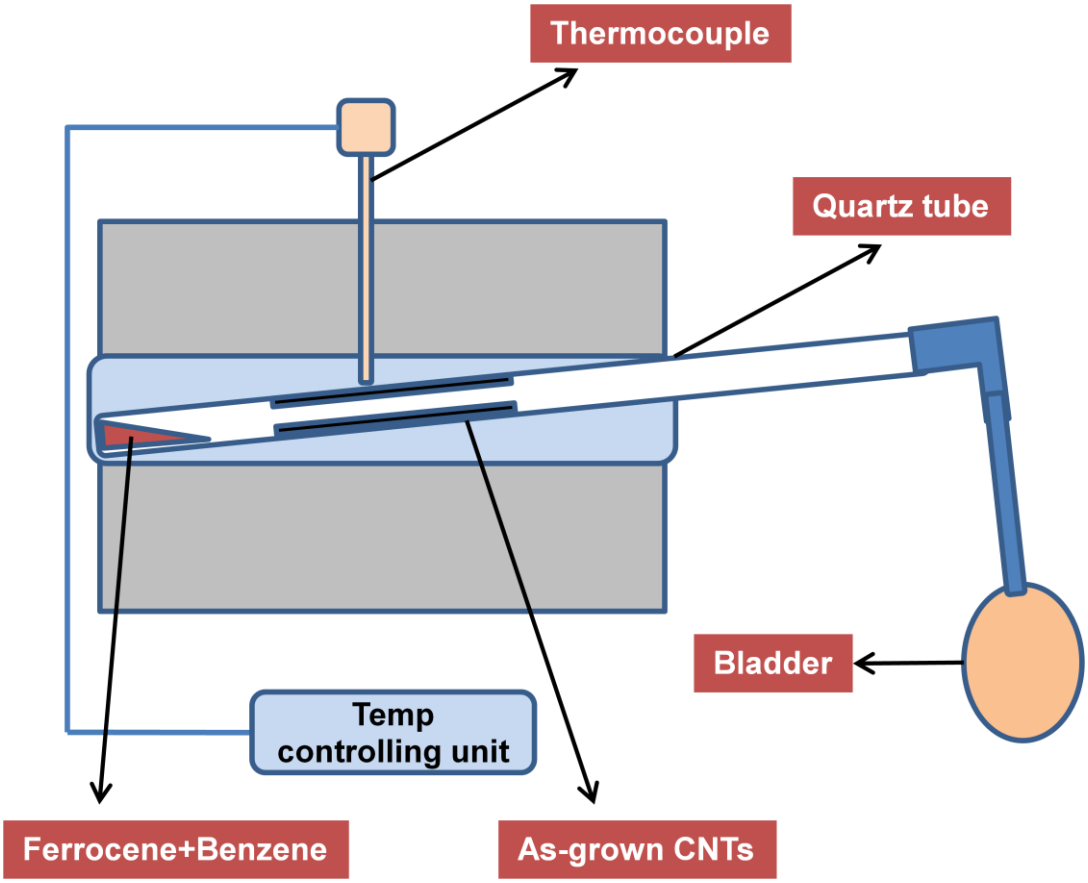

Figure 4: Schematic diagram of single hot-zone pyrolysis assisted chemical vapor deposition setup.

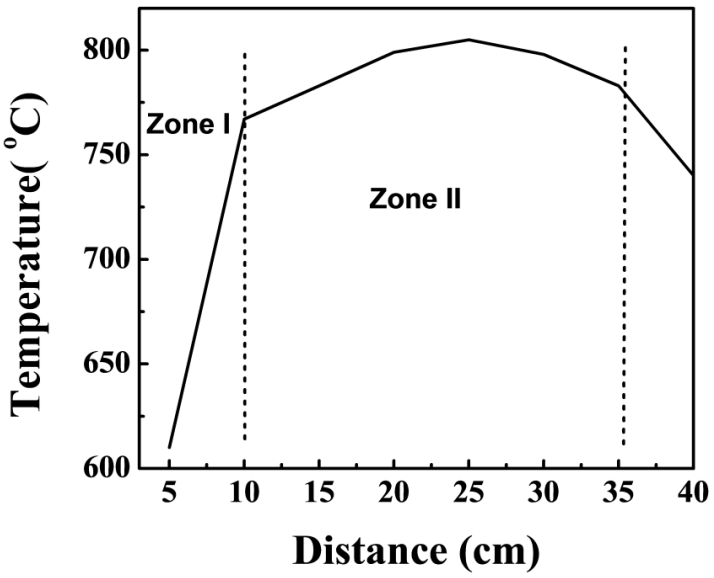

Figure 5: Temperature profile of the furnace used for the pyrolysis.

A mixture of 20 mg of ferrocene and 3 ml of benzene was placed into a quartz tube and the tube was kept inclined inside the furnace. The diameter and length of the quartz tube

are 22 and 720 mm, respectively. One end of the quartz tube is closed and a rubber bladder is connected at the other open end. The bladder is used to collect the residual gases from the quartz tube and also to carry out the reaction within a controlled atmosphere. The quartz tube was placed inside the furnace and the furnace was heated to the desired pyrolysis temperature (750-900°C). When the center of the hot zone reaches the desired temperature (800°C), the precursor end of the furnace is at 600°C. Due to this, vapors reaching zone II, thermally fragment into active carbon species and catalytic particles. When the carbon species and catalytic particles come into contact carbon nanotubes are formed. The as-prepared CNTs are impure in nature, which consist of carbonaceous impurities such as amorphous carbon and some traces of transition metal. The transition metal impurity present in the as-prepared black powder is due to the unreacted catalyst (i.e., ferrocene). CNT yield in the range of 200-300 mg was obtained for different temperatures. Pure CNTs are required in order to explore their enormous potential applications. The important procedures for the purification of CNT are filtration method [21], chromatography [22], gas phase oxidation [23] and acid oxidation [24]. We have followed the gas phase oxidation and subsequent acid treatment method to purify the as-synthesized CNT. The as-prepared and the purified CNTs were characterized using micro-Raman and FESEM techniques.

A DILOR-JOBIN-YVON-SPEX integrated Raman spectrometer (Model Labram) was used in the present study. The spectrometer consisted of a microscope coupled confocally to a 300 mm focal length spectrograph equipped with two switchable gratings (300 and 1800 grooves/mm). A HeNe 20 mW laser beam was used as the excitation source. The laser was totally reflected by a notch filter towards the sample under a microscope and the Raman scattering was totally transmitted through the notch filter towards the confocal hole and entrance slit of the spectrometer. The spectrum was recorded in a Peltier cooled charge coupled devices detector. The data were collected with a 20 s data point acquisition

time in the spectral range of 50-3000 cm^{-1}. The morphology, purity and the tube diameter of the CNTs were studied using Carl Zeiss Supra 40 VP FESEM.

3. Results and Discussion

CNTs were prepared at different temperatures in the range of 750-900°C without varying the ferrocene and benzene concentrations. After the experiment, the inner wall of the quartz tube at reaction zone II was found to be covered uniformly with a black residue. The black deposit in the form of flakes of sizes ranging from 2 to 10 mm and weighing 250-300 mg was taken out carefully. The collected black residue consists of CNTs and various other carbon species such as fullerenes, graphitized carbon nanostructures as well as amorphous carbon.

3.1. Microstructural studies of as-prepared CNTs

FESEM micrographs of carbon nanotubes prepared at different temperatures are shown in Figure 6. The CNTs observed at different temperatures were MWNTs with diameters in the range of 35-100 nm. The lengths of the CNTs observed at different temperatures were in the range of 10-25 µm. A typical cross-section of the vertically grown CNTs is shown in Figure 7 wherein the length of the CNT was found to be 25 µm. The FESEM data clearly showed the presence of impurities in the as-prepared CNTs which are seen as white regions. This was also confirmed by the micro-Raman spectroscopy data.

3.2. Micro-Raman spectroscopy studies

Raman spectroscopy is an important tool to characterize all sp^2 carbons such as graphite, graphene, CNT and fullerenes. The Raman spectroscopy data not only provides unique vibrational and crystallographic information, but also unique information about physical properties that are relevant to electrons and phonons [25]. The most prominent Raman features in CNTs are the radial breathing modes (RBMs), ‘D’, ‘G’ (graphite) and G′ modes.

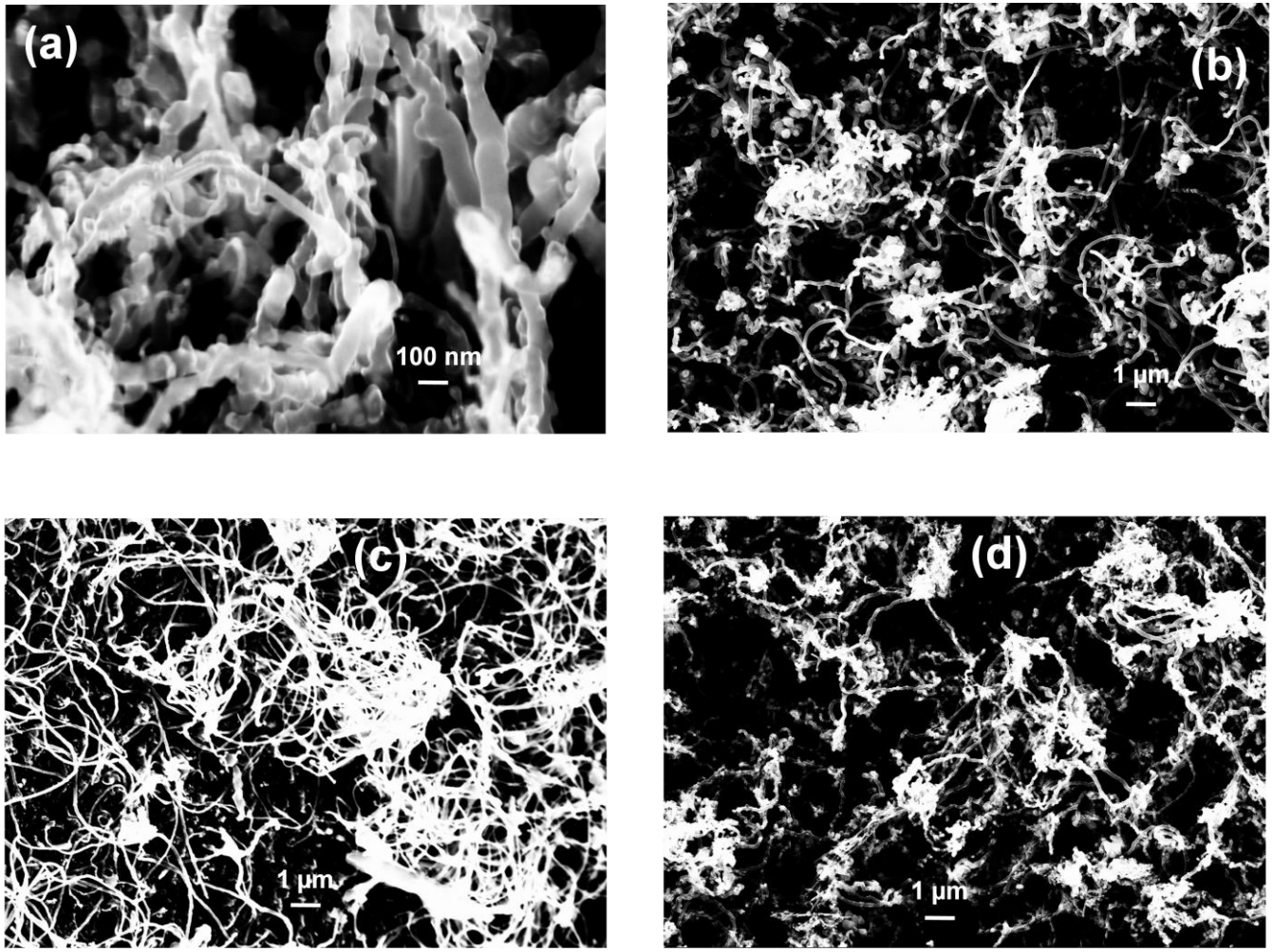

Figure 6: FESEM micrographs of as-prepared MWNTs synthesized at different temperatures (a) 750°C, (b) 800°C, (c) 850°C and (d) 900°C.

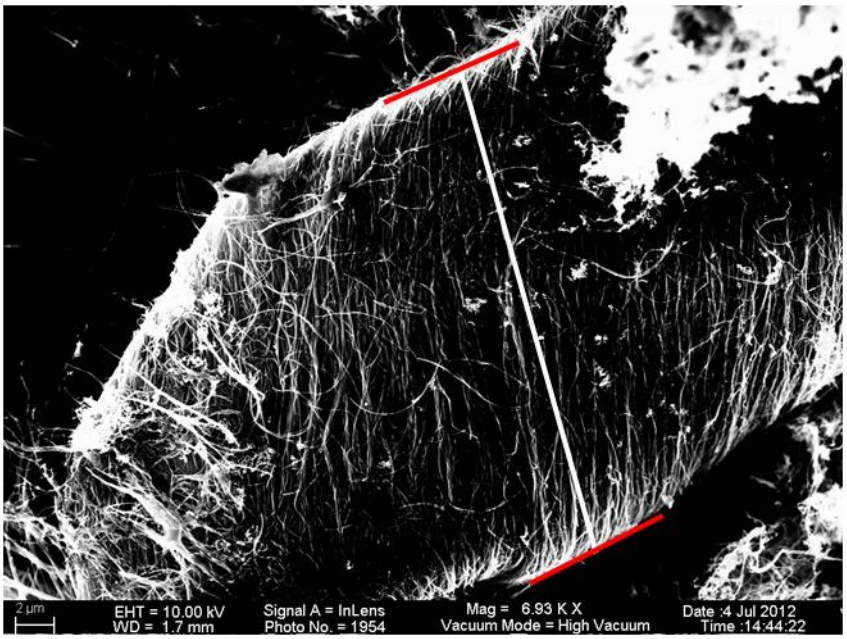

Figure 7: Typical cross-section of the vertically grown carbon nanotubes.

The 'G' band is the primary Raman active mode in graphite and it provides a good representation of the sp^2 bonded carbon of CNTs. The 'D' band known as the 'disorder' or 'defect' mode originates from edge configurations in graphene, where the planar sheet configuration is disrupted. The G′ band or 2D band is an overtone mode of the D-band. The cylindrical shape of the CNT introduces another Raman feature, the radial breathing mode, wherein each atom in the CNT is vibrating in the radial direction. The RBM frequency is inversely proportional to the diameter, making it an important feature for determining the diameter distribution in a sample.

A typical micro-Raman spectrum of as-prepared multi-walled carbon nanotubes prepared at 850°C is shown in Figure 8. The Raman spectrum showed three peaks at 1330, 1585 and 2661 cm^{-1}, which correspond to D, G and G′ bands, respectively [20]. The D peak at 1330 cm^{-1} is due to the presence of amorphous carbon in the as-prepared CNT. The peak at G band indicates the presence of highly crystalline graphitic layers. The G′ band frequency is twice that of the D band and this band is an intrinsic property of the nanotube.

The intensity ratio I_D/I_G is used to characterize the degree of the carbon materials, i.e., smaller ratio of I_D/I_G corresponds to higher degree of CNT formation [26]. The I_D/I_G intensity ratio is high (Figure 8) which confirms that some amount of impurity is present in the as-prepared CNTs. In order to obtain pure CNTs, the as-prepared CNTs were purified by gas phase oxidation method followed by the hydrochloric acid-treatment.

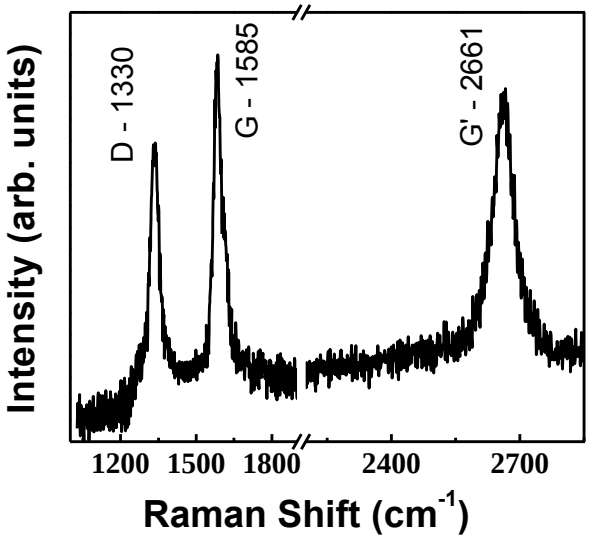

Figure 8: A typical Raman spectrum of as-prepared multi-walled carbon nanotubes prepared at 850°C.

3.3. Purification of CNT

In gas phase oxidation, the etching of amorphous carbon takes place from the surface of the CNTs and the catalyst particles present in the sample. The carbonaceous particles are removed during gas phase oxidation in air or oxygen, since the etching rate of the amorphous carbon is faster than CNTs [20]. However, gas phase oxidation cannot eliminate the transition metals present in the as-synthesized CNTs. Therefore, liquid phase reactions in various acids are further necessary in order to melt away the transition metals.

The as-prepared CNTs synthesized at 850°C were oxidized in air at 500°C for 3 hrs. After the oxidation, the CNTs were soaked in 6M HCl for 12 hrs. The acid treated sample was washed many times in deionized water to remove the acid. The final product was recovered by drying in the oven after the material is filtered out. FESEM and micro-Raman spectroscopy techniques were used to confirm the purity of CNTs. Figure 9 shows the FESEM micrographs of impure CNT (as-prepared at 850°C, Figure 9(a)), CNT obtained after oxidation at 500°C (Figure 9(b)) and CNT obtained after chemical etching with HCl (Figure 9(c)). The same procedure was followed to purify the as-prepared CNTs synthesized at temperatures in the range of 750-900°C, and the FESEM micrographs of purified CNT are shown in Figure 10. The Raman data of the purified CNT (prepared at 850°C) confirmed the presence of high purity CNT as shown in Figure 11. The I_D/I_G ratio of the purified CNT is 0.52, whereas, for the as-prepared CNT the ratio is 0.88 (see Figs. 8 and 11). The intensity ratio reduced drastically which confirms the presence of high purity CNTs.

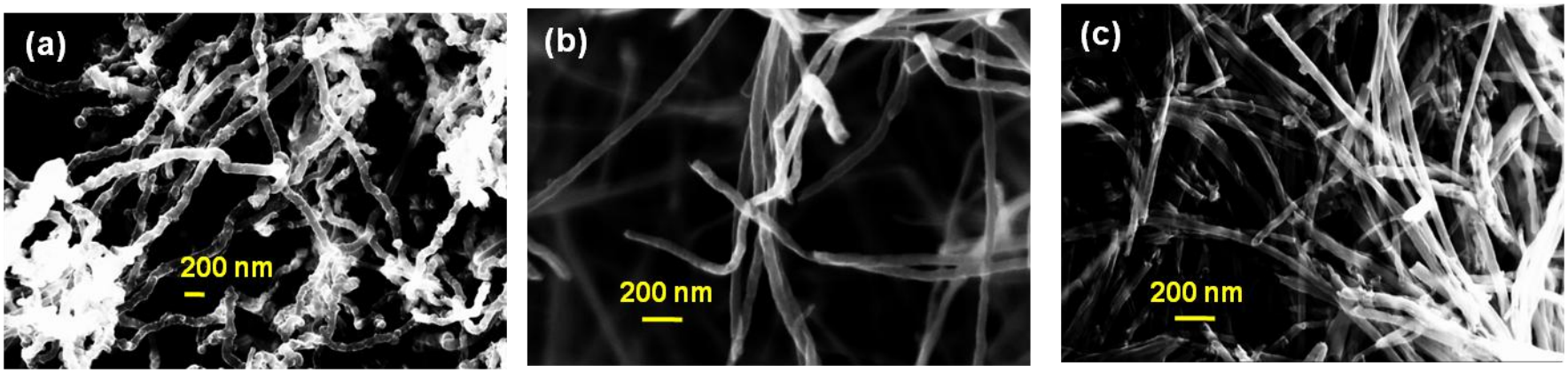

Figure 9: FESEM images of (a) as-prepared CNT at 900°C; (b) after oxidation at 500°C and (c) after chemical etching with HNO_3.

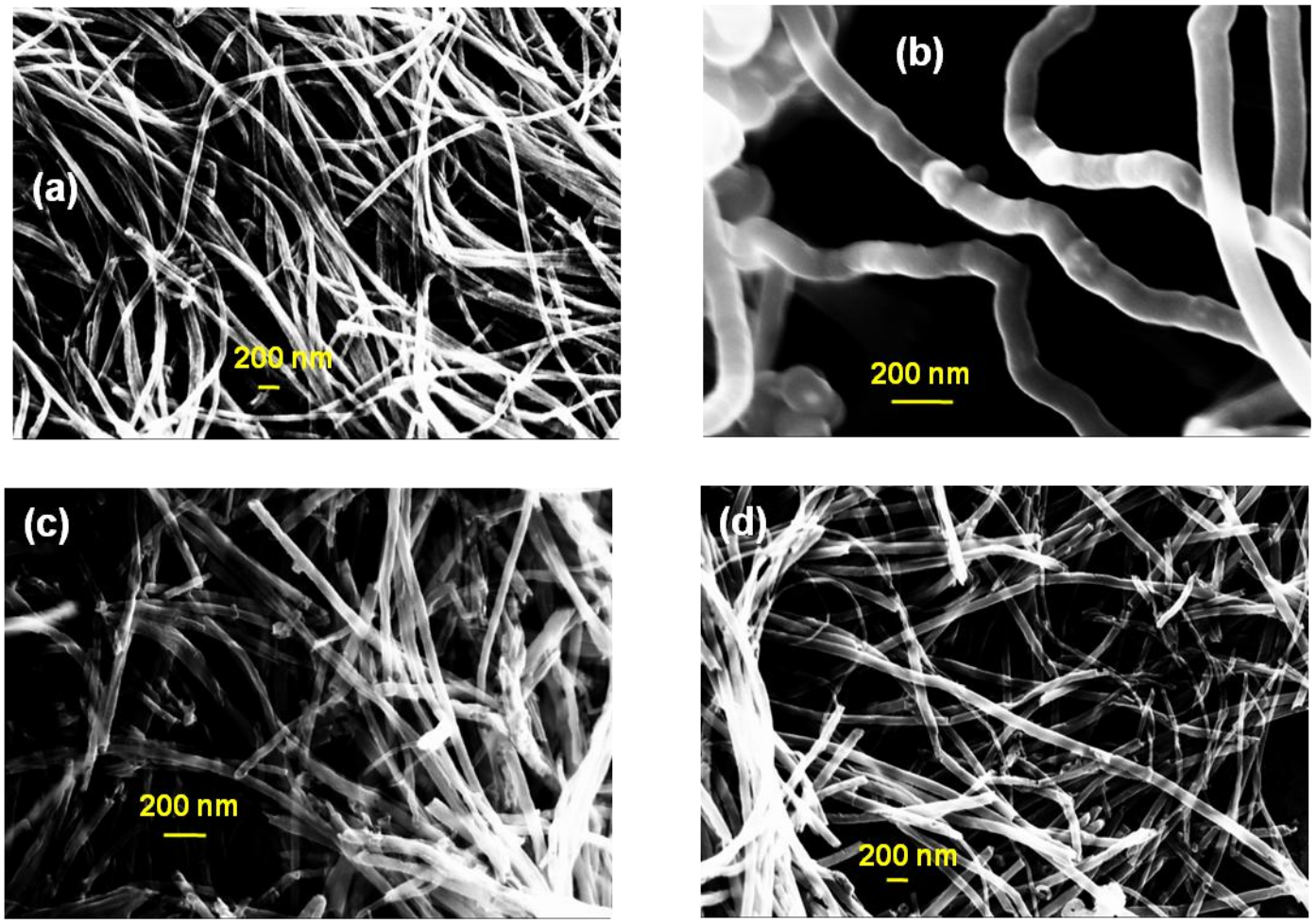

Figure 10: FESEM images of pure multi-walled CNTs prepared at different temperatures (a) 750°C, (b) 800°C, (c) 850°C and (d) 900°C.

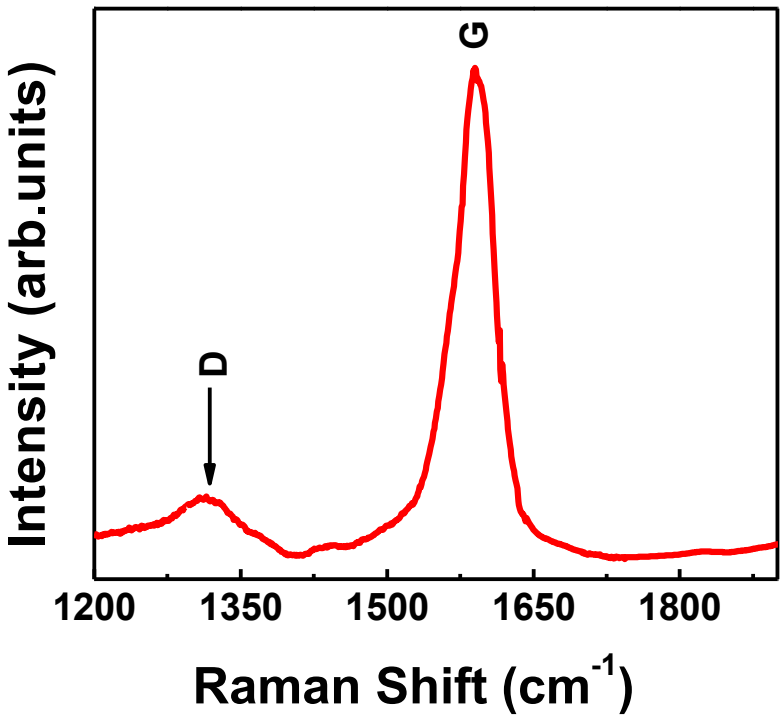

Figure 11: Typical Raman spectrum of purified CNT for the sample prepared at 850°C.

4. Conclusions

Carbon nanotubes were synthesized in a quartz tube by a single zone pyrolysis technique using ferrocene as a catalyst and benzene as a carbon precursor. CNTs were grown at different temperatures in the range of 750-900°C. The CNTs prepared at different temperatures were mutli-walled with diameter in the range of 35-100 nm. The FESEM micrographs clearly showed the presence of impurities in the as-prepared sample, which was also confirmed by the micro-Raman spectroscopy studies. The Raman data showed peaks corresponding to D, G and G′ modes of carbon nanotube. However, the high I_D/I_G ratio indicated the presence of impurities in the as-prepared sample. The CNTs were purified by gas phase oxidation followed by hydrochloric acid treatment for 12 hrs. The purity of the CNT was confirmed by micro-Raman spectroscopy studies which showed a drastic reduction in the D peak intensity. Further, the I_D/I_G ratio was very low for the purified sample clearly indicating the high purity of the CNT.

Acknowledgements

The authors thank Head, SED for various supports and Director, NAL (CSIR) for giving permission to publish these results.

References

1. M.S. Dresselhaus, G. Dresselhaus, P. Avouris (Eds.), Carbon nanotubes: synthesis, structure, properties and applications, vol. 80, Springer-Verlag, Heidelberg, Germany, 2001 (Topics in Applied Physics).
2. J. Han and C. Gao, Nano-Micro Letters 2 (2010) 213.
3. H. Kim, A.A. Abdala and C.W. Macosko, Macromolecules 43 (2010) 6515.
4. W. Liang et al., Nature 411 (2001) 665.
5. P. Kim, L. Shi, A. Majumdar, P.L. McEuen, Phys. Rev. Lett. 87 (2001) 215502.
6. G. Gao, T. Cagin, W.A. Goddard, Nanotechnology 9 (1998) 184.
7. G. Baumgartner et al., Physical Review B 55 (1997) 6704.
8. J. Hone et al. Science 289 (2000) 1730.
9. S.P. Frank, P. Poncharal, Z.L. Wang, W.A. de Heer, Science 280 (1998) 1744.
10. A. Hagen and T. Hertel, Nano Letters 3 (2003) 383.
11. J.A. Misewich, R. Martel, Ph. Avouris, J.C. Tsang, S. Heinze and J. Tersoff, Science 287 (2000) 637.
12. T.W. Ebbesen, P.M. Ajayan, Nature 358 (1992) 220.
13. A. Thess, R. Lee, P. Nikolaev, H. Dai, P. Petit, J. Robert, C. Xu. Y.H. Lee, S.G. Kim etal. Science 273 (1996) 483.
14. Y. Kim, C.M. Yang, Y.S. Park, K.K. Kim, S.Y. Jeong, J.H. Han, Y.H. Lee, Chemical Physics Letters 413 (2005) 135.
15. K.H. Jung, J.H. Boo, B. Hong, Diamond Related Materials 13 (2004) 299.
16. S. Bondi, W.J. Lackey, R.W. Johnson, X. Wang, Z.L. Wang, Carbon 44 (2006) 1393.
17. G. Nasibulin, A. Moisala, H. Jiang and E.I. Kauppinen, Journal of Nanoparticle Research 8 (2006) 465.
18. L. Jiang and L. Gao, Chemical Materials 15 (2003) 2848.

19. P. Nikolaev, M.J. Bronikowski, R.K. Bradley, F. Rohmund, D.T. Colbert, K.A. Smith, R.E. Smalley, Chemical Physics Letters 313 (1999) 91.

20. P. Mahanandia, P.N. Vishwakarma, K.K. Nanda et al., Solid State Communications 145 (2008) 143.

21. K.B. Shelimov, R.O. Esenaliev, A.G. Rinzler, C.B. Huffman, R.E. Smalley, Chemical Physics Letters 282 (1998) 429.

22. E. Farkas, M.E. Anderson, Z.H. Chen, A.G. Rinzler, Chemical Physics Letters 363 (2002) 111.

23. J.M. Moon, K.H. An, Y.H. Lee, Y.S. Park, D.J. Bae and G.S. Park, Journal of Physical Chemistry B 105 (2001) 5677.

24. Y. Wang, Y.Q. Liu, D.C. Wei, L.C. Cao et al. Journal of Materials Chemistry 17 (2007) 357.

25. L.M. Malard, M.H.D. Guimares, D.L. Mafra, M.S.C. Massoni and A. Jorio, Physical Review B 79 (2009) 125426.

26. S.S. Xie, W.Z. Li, Z.W. Pan, B.H. Chang and L.F. Sun, European Physics Journal D 9 (1999) 85.